 DOI: 10.1002/masy.201000056

Quantum Chemistry: A Powerful Tool in Polymer Reaction Engineering

*Marco Dossi, Giuseppe Storti, Davide Moscatelli**

Summary: The potentials of computational techniques based on quantum mechanics, to support and complement the experimental analysis, are examined. Mechanisms and reaction paths involved in the free radical polymerization of widely used monomers are studied through a computational approach based on Density Functional Theory (DFT). First, the attention is focused on the initiation kinetics in order to evaluate the role of the initiators in the polymerization process. Methyl acrylate, methyl methacrylate, acrylonitrile, and styrene homopolymerization using different initiators are studied. Then, propagation kinetics is investigated. In particular, the propagation kinetic rate constants for different kinds of acrylates, methacrylates and acetates are calculated and compared with experimental data reported in the literature. The same computational approach is applied to the study of secondary reactions (backbiting, beta-scission) occurring during free radical polymerizations. Finally, the same methodologies are applied to copolymer systems, with emphasis on the evaluation of the role of penultimate effect. The copolymers vinyl acetate/methyl methacrylate and styrene/methyl methacrylate are investigated as system characterized by weak and strong penultimate effect, respectively.

Keywords: copolymer; kinetics; modeling; polymerization; quantum chemistry

Introduction

In the last decades, remarkable efforts and considerable progresses have been made in polymer reaction engineering to obtain reliable and accurate kinetic information by different experimental methods.[1] With reference to the free radical polymerizations, thanks to the assessment of sophisticated experimental techniques such as Pulsed Laser Polymerization combined with Size Exclusion Chromatography (PLP-SEC), thermodynamic and kinetic parameters can be directly and accurately evaluated.[2] However, the experimental determination of rate coefficients is often time consuming or very complicated to achieve, mainly because the separate study of a specific kinetic step out of all the possible reactions is practically impossible.[3]

Keeping this scenario on the background, theoretical predictions of kinetic properties based on Quantum Mechanics (QM) methods could be represent a powerful tool to support and enrich the experimental efforts.[1d,4] With the aim to identify the capabilities of such computational techniques, in this work mechanisms and reaction paths involved in the free radical polymerization of widely used monomers are studied through an approach based on Density Functional Theory (DFT).

Having in mind the most conventional kinetic scheme of free radical polymerization,[5] the analysis is first focused on initiation kinetics, i.e. the reaction of the first monomer unit with the initiator fragment. The experimental evaluation of such rate constants is difficult because such reaction step is usually faster than the propagation one. Different monomers of industrial relevance such as methyl-acrylate

Dipartimento di Chimica, Materiali e Ingegneria Chimica "Giulio Natta", Politecnico di Milano, 20131 Milano, Italy
E-mail: davide.moscatelli@polimi.it

(MA), methyl-methacrylate (MMA), acrylonitrile (AN) and styrene (ST) are studied in free-radical polymerization initiated by five widely used initiators, exhibiting different behaviors in terms of water solubility and dissociation mechanism: azobis-isobutyronitrile (AIBN), di-tert-butyl peroxide (DTBP), potassium persulfate (KPS), 2,2-dimethoxy-2-phenyl acetophenone (DMPA) and dibenzoyl peroxide (DBP).

Then, the propagation kinetics of eight different systems is evaluated, i.e. the reaction of the monomer unit with a long active chain. In particular MA, ethyl acrylate (EA), butyl acrylate (BA) are considered as monomers representative of the acrylate group, MMA and 2-hydroxyethyl methacrylate (HEMA) of the methacrylate group and vinyl acetate (VAc) of the acetate group. Moreover, ST and acrylonitrile (AN) are also included in the investigation of propagation kinetics.

According to most conventional kinetic scheme of free radical polymerization, the next step to be analyzed is termination.[5] However, this reaction step is mainly controlled by diffusion and the proposed computational approach is indeed not best suited to investigate it.

The third application of the computational method here proposed focuses on the so-called secondary reactions. Their relevance as events responsible of the mid-chain radicals (MCRs) formation, was recently proved.[6–8] The experimental evaluation of kinetic parameters typical of these reactions is very complicated to achieve even through the most advanced techniques, due to the reactivity differences between secondary and tertiary carbon radicals.[2g] The case of vinyl chloride (VC) is examined in comparison with cases of ST and AN previous studied,[4f,4n] while 1:3, 1:5, and 1:7 backbiting reactions, and the right and left beta-scissions from the mid chain radicals (MCRs) formed by such backbiting reactions, are analyzed as representative secondary reactions.

Finally, the methodology based on the DFT theory is applied to copolymer systems. The analysis has been finalized to show the capabilities of this computational approach to reproduce composition data and, most important, copolymer propagation kinetics. In particular the differences between terminal[9] and penultimate models[10] are analyzed examining two limiting cases: VAc/MMA copolymer, exhibiting a weak penultimate unit effect,[11] and ST/MMA copolymer, characterized by a strong penultimate unit effect.[10]

Computational Details

As mentioned in the Introduction, all the kinetic parameters are evaluated adopting the DFT. In particular the Becke 3 parameter and Lee-Yang-Parr functional (B3LYP) are used in the DFT calculations to evaluate exchange and correlation energies. [12,13] All quantum chemical calculations of reactants and products have been performed with a spin multiplicity of 2 using an unrestricted wave function in order to avoid spin contamination (UB3-LYP). Previous works reported in the literature demonstrate that B3LYP methods provide excellent low-cost performance, leading to computational results in good agreement with the experimental data.[1d,4d,4l,4m,14–17] The all electron 6-31 basis set with added polarization functions (6-31G(d,p)) is used for the basis set.

''Long chains'' are simulated as made of three monomer units, assuming $k_{p,3} \simeq k_{p,\infty} \equiv k_p$ as mentioned in previous papers.[4e,4i,4m] Only in the study of backbiting and beta-scission reactions, radical chains composed by six monomer units are simulated.

All geometries are fully optimized with the Berny algorithm and are followed by frequency calculations. The geometry of each molecular structure is considered stable only after calculating vibrational frequencies and force constants and only if no imaginary vibrational frequency was found. Transition state structures are located adopting the synchronous transit-guided quasi Newton method and are characterized by a single imaginary vibrational frequency.[18]

Kinetic constants are determined through the classical transition state theory (TST) as:

$$k(T) = A \cdot e^{-Ea/k_b T} = \frac{k_b T}{h} \cdot \frac{q_{\neq}^{rot} q_{\neq}^{vib} q_{\neq}^{el}}{\prod_{reactants} q^{rot} q^{vib} q^{el}} \cdot e^{-Ea/k_b T} \quad (1)$$

where k_b and h are Boltzmann and Plank constant, respectively, T is the temperature, E_a is the activation energy of the process, and $q_{\neq}^{vib}, q_{\neq}^{rot}, q^{vib}, q^{rot}$ are the vibrational and rotational partition functions for transition states and reactants.

Partition functions are built using the independent harmonic-oscillator (HO) approximation. In fact, even if the computational accuracy is improved by treating the low frequency torsional modes as internal rotations,[4a,4b,19] it was also shown that the corrections of the partition functions can be more or less critical depending upon the specific system under investigation.[1d,19–21] All quantum chemistry calculations are performed with the Gaussian 03 suite of programs and all pictures are drawn with PyMol 1.3.[22,23]

Results and Discussion

Initiation Kinetics

The results summarized in this section are part of a previously published comprehensive study on initiation kinetics in free radical polymerization.[4m] The initiation step in the polymerization of MA, MMA, AN, and ST was investigated using several different initiators: AIBN, DTBP, KPS, DMPA and DBP. AIBN is a fat-soluble initiator decomposing into two 2-cyanoprop-2-yl radicals (AIBN·). DTBP is an initiator slightly soluble in water that produces two tertbutyloxy radicals (t-but-O·). KPS is a very popular, water soluble initiator that produces two sulfate anion-radicals (SO_4^-·).[24] DMPA is a water-insoluble photoinitiator that leads to one benzoyl radical (PhO) and one methyl radical (Me) by a multi-step photolytic mechanism.[25] DBP is oil-soluble and decomposes into carbon dioxide and two phenyl radicals (Ph).

The combinations involving radical fragments, coming from the initiator decompositions, and all the monomers above were systematically studied, and the corresponding rate constants, k_I, were calculated. The resulting values are collected in Table 1 together with the values of the corresponding propagation rate constants (i.e. the rate constants of each monomer with its own long-chain radical) as reported in the literature. All the kinetic parameters were calculated at 28 °C.

According to the values in Table 1, the initiator largely affects the kinetics of the first reaction step: depending upon the type of initiator, the rate constant values of the reaction between the initiator fragment and the first monomer unit are from one to six orders of magnitude larger than the long-chain propagation rate constant of the same monomer. In all cases, the initiator reactivity decreases from DBP to AIBN while DTBP, KPS and DMPA exhibit intermediate reactivity.

Table 1.
Comparison between kinetic rate constants for initiation reactions (k_i) and experimental values of the rate constant for long-chain propagation (k_p) of all monomers. Kinetic parameters at 28 °C. All values are in L/mol/s.

		Monomer			
		MA	MMA	AN	St
k_i	AIBN·	$2.12 \cdot 10^0$	$2.47 \cdot 10^0$	$4.26 \cdot 10^0$	$4.35 \cdot 10^0$
	t-but-O·	$1.02 \cdot 10^4$	$6.84 \cdot 10^4$	$2.11 \cdot 10^4$	$2.44 \cdot 10^5$
	SO_4^-·	$8.85 \cdot 10^5$	$3.38 \cdot 10^6$	$9.04 \cdot 10^5$	$4.88 \cdot 10^5$
	PhO	$1.97 \cdot 10^5$	$2.56 \cdot 10^5$	$5.22 \cdot 10^4$	$1.34 \cdot 10^4$
	Me	$1.76 \cdot 10^7$	$2.71 \cdot 10^7$	$1.56 \cdot 10^6$	$2.07 \cdot 10^6$
	Ph	$1.70 \cdot 10^8$	$1.67 \cdot 10^8$	$1.85 \cdot 10^8$	$9.77 \cdot 10^7$
k_p		$1.41 \cdot 10^4$ [26]	$3.39 \cdot 10^2$ [27]	$3.79 \cdot 10^3$ [28]	$9.79 \cdot 10^1$ [2c]

Propagation Kinetics

This step is the most important one in polymerization reactions, playing a paramount role in determining the molecular weight distribution of the final polymer and thus the final properties of the product.

As mentioned in the Introduction, the propagation kinetics of free radical homopolymerization own of different polymeric systems was computationally examined. In particular, activation energy and frequency factor values were calculated for MA, EA, BA, MMA, HEMA, VAc, AN and ST and compared to the corresponding values proposed in literature. All the resulting values are collected in Table 2. Moreover, propagation rate coefficients at a specific temperature are also reported in Table 2, with the aim to help the comparison between experimental and computational parameters. The optimized molecular geometries involved in the propagation step for EA are shown in Figure 1, as representative of the simulations performed. In order to compare computational and experimental results, the activation energy was considered independent upon the temperature, while the frequency factor, and as a consequence propagation rate coefficient, was evaluated for each system at the temperature considered in the reference literature work.

Data in Table 2 indicate a generally good agreement between computational and experimental results. This agreement is particularly satisfactory in terms of activation energy values: as a matter of fact computational method reproduces the literature values with an absolute error smaller than 2 kcal/mol. In terms of frequency factor, larger discrepancy arise, especially for MA, MMA and AN. Taking into consideration propagation rate coefficient values, the most relevant divergence is observable for VAc. Concerning other systems, computational propagation rate coefficient differs by two or three times maximum from the experimental one, indicating the method proposed as a semi-quantitative tool for reasonable first-guess values prediction.

Secondary Reactions

Beyond the well assessed initiation and propagation reactions, other kinetic steps affect the final properties of the polymer at a significant extent. Especially, MCRs can be formed by backbiting reactions, thus introducing anomalous behaviors into the process of chain growth. The relevance of such phenomena has been recently discussed.[3,4f]

Due to the difficulties involved in the direct experimental analysis of such reactions, the application of the DFT approach represents a invaluable tool in the study of these unconventional reactions. In particular secondary reactions involved in styrene and acrylonitrile homo-polymerization were computationally studied in our previous works.[4f,4n] Recently we extended the same investigation to the polymerization of

Table 2.
Comparison between Arrhenius propagation parameters for MA, EA, BA, MMA, HEMA, ST, VAc and AN, both theoretically and experimentally determined. Activation energies (E_a) in kcal·mol^{-1}, frequency factors (A) and k_p in L·mol^{-1}·s^{-1}. $k_p = A \cdot exp(-E_a/R/T)$. The notation k_p^* indicates that the computation examines monomer addition to a dimeric radical.

Monomer	$\log_{10}(A)$	E_a	k_p^*	ref.	$\log_{10}(A)$	E_a	k_p	ref.
		(computational)				(experimental)		
MA (25 °C)	8.55	6.54	5666	this work	7.22	4.23	13152	[26]
EA (40 °C)	8.44	6.46	8491	this work	–	–	4700	[29]
BA (20 °C)	8.36	6.24	5072	this work	7.34	4.28	14476	[2g]
MMA (40 °C)	8.01	7.91	307	this work	6.43	5.34	502	[27]
HEMA (100 °C)	7.10	6.39	2268	1d	6.95	5.23	7680	[30]
ST (40 °C)	8.42	8.29	428	this work	7.63	7.77	161	[2c]
VAc (25 °C)	7.34	3.71	41582	this work	7.16	4.94	3442	[31]
AN (25 °C)	8.74	7.51	1705	4h	6.25	3.68	3562	[28]

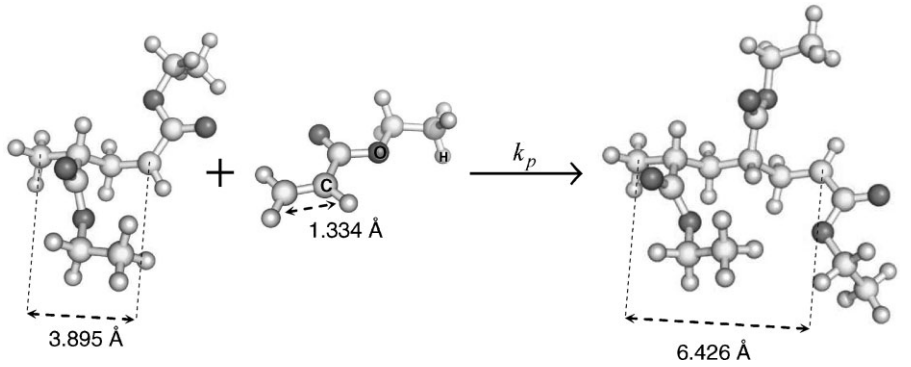

Figure 1.
Optimized molecular geometries involved in the simulated propagation reaction for ethyl acrylate.

vinyl chloride,[32] because in this system the presence of MCRs leads to the formation of chain defects which affect the major applicative properties of the final polymer.[33]

In this section of the present work, some of the results obtained in the study of poly-VC (PVC) are reported with the aim to compare these new findings with data already published on ST and AN. In particular two types of secondary reactions, backbiting and beta-scission, are here discussed: the 1:3, 1:5 and 1:7 backbiting reactions, corresponding to hydrogen transposition from the position 3, 5, and 7, respectively, to position 1 in the active chain, and the right and left beta-scissions from the formed mid chain radicals.

The calculated kinetic parameters for the PVC backbiting reactions are collected in Table 3, while those for the beta-scission reactions are shown in Table 4. Moreover, to facilitate the comparison between the three systems, data related to ST and AN are also summarized in the same tables.

According to the numerical values in the tables, similar trends in behavior of investigated systems are observed, and the same conclusion obtained in our previous computational studies on backbiting and

Table 3.
Arrhenius parameters for 1:3, 1:5 and 1:7 hydrogen transpositions for PVC, ST and AN radical chains. Activation energies (E_a) in kcal·mol^{-1}, frequency factors (A) in s^{-1} and $k_{bb} = A \cdot T \cdot \exp(-E_a/RT)$.

	k_{bb} – PVC		k_{bb} – ST[4f]		k_{bb} – AN[4n]	
	$\log_{10}A$	E_a	$\log_{10}A$	E_a	$\log_{10}A$	E_a
$R_{n,1} \rightarrow R_{n,3}$	10.26	38.25	11.34	41.30	9.68	37.85
$R_{n,1} \rightarrow R_{n,5}$	9.13	17.11	10.77	17.92	8.81	17.75
$R_{n,1} \rightarrow R_{n,7}$	8.47	24.19	11.62	21.70	8.16	23.65

Table 4.
Arrhenius parameters for both right and left beta-scission reactions of PVC, ST and AN MCRs. Activation energies (E_a) in kcal·mol^{-1}, frequency factors (A) in s^{-1} and $k_{bb} = A \cdot T \cdot \exp(-E_a/RT)$.

	PVC				ST[4f]				AN[4n]			
	$k_{\beta\text{-}s}$ (right)		$k_{\beta\text{-}s}$ (left)		$k_{\beta\text{-}s}$ (right)		$k_{\beta\text{-}s}$ (left)		$k_{\beta\text{-}s}$ (right)		$k_{\beta\text{-}s}$ (left)	
	$\log_{10}A$	E_a	$\log_{10}A$	E_a	$\log_{10}A$	E_a	$\log_{10}A$	E_a	$\log_{10}A$	E_a	$\log_{10}A$	E_a
$R_{n,3}$	10.81	30.30	9.70	27.20	12.72	22.50	12.71	20.63	10.56	26.27	11.56	22.64
$R_{n,5}$	10.55	25.46	10.24	24.89	12.74	20.00	12.74	20.00	10.87	23.49	10.66	23.40
$R_{n,7}$	10.27	24.77	10.19	25.28	12.49	24.02	12.49	24.02	10.60	23.43	10.31	22.67

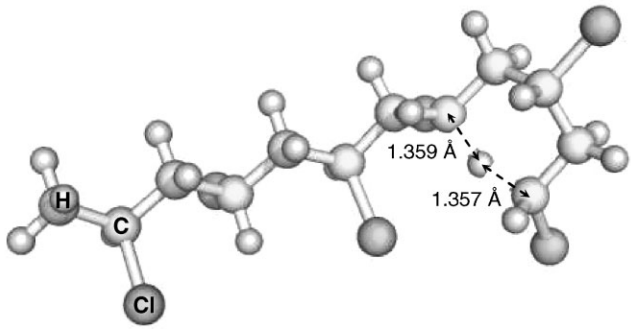

Figure 2.
Transition state geometry for the Poly-Vinyl Chloride 1:5 backbiting reaction calculated with computational approach. Distances are reported in angstroms (syndiotactic molecular model).

beta-scission reactions[4f,4n] is confirmed even for PVC. Namely the 1:5 hydrogen transpositions is the most favorite, while the activation energy values increase from backbiting 1:7 to 1:3. These results may be explained in terms of transition state stability: in fact, the 1:5 backbiting reactions lead to the formation of a six member ring transition state characterized by low internal strain (Figure 2). About the beta-scission reactions, the kinetic parameters seem to be weakly related to the scission position, right or left, and slightly dependent upon the position of the mid chain radical in the chain, 3, 5 or 7. The only exception is represented by the right beta-scission occurring in chains with the radical in position 3, most probably due to the formation of an instable small radical fragment, as shown in Figure 3.

Copolymerization Reactions

The aim of the last section is to explore the capabilities of the computational methodologies under examination to investigate copolymeric systems, in particular providing insight into the propagation reactions, i.e. pointing out molecular differences between very popular kinetic models such as the terminal[9] and penultimate models.[10]

In a previous work, the copolymer vinyl acetate/methyl methacrylate has been investigated using the same computational model.[41] Small deviations from the terminal model for this copolymer system were reported in the literature[12] and a weak penultimate effect was in fact confirmed by our simulations. The computational[41] and experimental[12] parameter values for the copolymerization model, both terminal

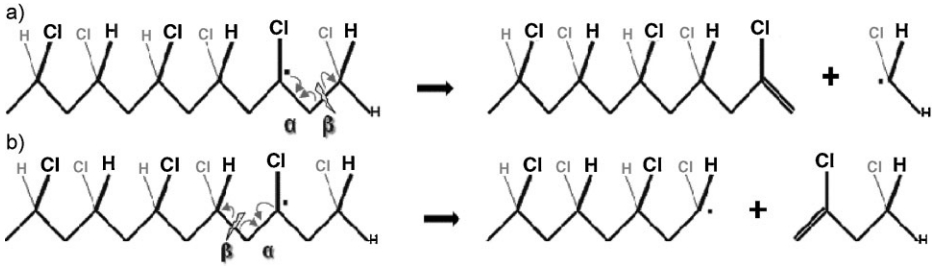

Figure 3.
Poly-Vinyl Chloride beta-scission reaction scheme. Right (a) and left (b) beta-scission from MCR with radical in position 3.

Table 5.
Computational[41] and experimental[12] parameter values for the copolymer VAc/MMA, both TM and IPUE. $r_1 = k_{p11}/k_{p12}$, $r_2 = k_{p22}/k_{p21}$, and k_{pij} is the propagation rate coefficient for addition of monomer-j to radical-i. $s_1 = k_{p211}/k_{p111}$, $s_2 = k_{p122}/k_{p222}$, and $k_{p,ijk}$ is the propagation rate coefficient for addition of monomer-k to a growing radical-j with unit-i in the penultimate position. (monomer 1 = vinyl acetate, monomer 2 = methyl methacrylate).

	Experimental T@40 °C	Computational T@40 °C
r_1	0.014	0.001
r_2	27.8	31.0
s_1	*	0.176
s_2	0.4 ± 0.2	0.538

*assumed equal to s_2

(TM) and implicit penultimate (IPUE),[10] are collected in Table 5.

In order to further confirm the validity of the method, the same procedure applied in the case of the copolymer VAc/MMA,[41] is extended here to the copolymer ST/MMA. This system was considered particularly interesting because exhibiting a strong penultimate effect.[10,34,35] In particular the copolymer composition conforms to the terminal model,[9] whereas the propagation rate constant measured experimentally are well represented by the implicit penultimate model.[10]

The kinetic parameters for both the copolymerization models, terminal and implicit penultimate, have been determined and all the calculated values are summarized in Table 6 along with the experimental ones.[10] Moreover, the copolymer composition (F_1) and copolymer propagation rate coefficients ($k_{p,cop}$), both as a function of ST monomer mole fraction (f_1), are compared to the experimental data in Figure 4 and Figure 5, respectively. In particular, the copolymer composition has been calculated through equation (2), while the copolymer propagation rate coefficients (TM and IPUE model) through equation (3) and equation (4). Of course, the predicted values of r_1, r_2, s_1 and s_2 have been used in all cases.

$$F_1 = \frac{r_1 f_1^{\,2} + f_1 f_2}{r_1 f_1^{\,2} + 2 f_1 f_2 + r_2 f_2^{\,2}} \tag{2}$$

$$\text{TM} \qquad k_{\text{p,cop}} = \frac{r_1 f_1^2 + 2 f_1 f_2 + r_2 f_2^2}{\left(r_1 \frac{f_1}{k_{11}}\right) + \left(r_2 \frac{f_2}{k_{22}}\right)} \tag{3}$$

$$\text{IPUE} \qquad k_{\text{p,cop}} = \frac{r_1 f_1^2 + 2 f_1 f_2 + r_2 f_2^2}{\left(r_1 \frac{f_1}{\overline{k_{11}}}\right) + \left(r_2 \frac{f_2}{\overline{k_{22}}}\right)} \tag{4}$$

where the new coefficients of the IPUE model are calculated as:

$$\overline{k_{11}} = k_{p111} \frac{r_1 f_1 + f_2}{r_1 f_1 + f_2/s_1}$$

$$\overline{k_{22}} = k_{p222} \frac{r_2 f_2 + f_1}{r_2 f_2 + f_1/s_2} \tag{5}$$

As showed in the Propagation kinetics section, the prediction of the absolute values of propagation rate coefficient relative to homopolymerization reactions is more or less accurate according to the system investigated. Moreover previous works well describe the major accuracy of these techniques to estimate relative rate coefficients compared to absolute values, mainly due to the approximation adopted in the computational analysis.[41,4k] To not introduce this uncertainty in the study of copolymerization propagation kinetics, the propagation rate coefficients for the homopolymerization of ST (k_{p111}) and MMA (k_{p222}), were taken from previous PLP-SEC studies.[2c,27]

Table 6.
Computational and experimental[10] parameter values for the copolymer ST/MMA, both TM and IPUE. (monomer 1 = styrene, monomer 2 = methyl methacrylate).

	Experimental T@40 °C	Computational T@40 °C
r_1	0.52	0.53
r_2	0.46	0.68
s_1	0.30	0.23
s_2	0.53	0.99

Values in Table 6 show a satisfactory agreement between computational and experimental results. Moreover, the curves calculated using the computational parameter values fit with good accuracy to the experimental data for both copolymer

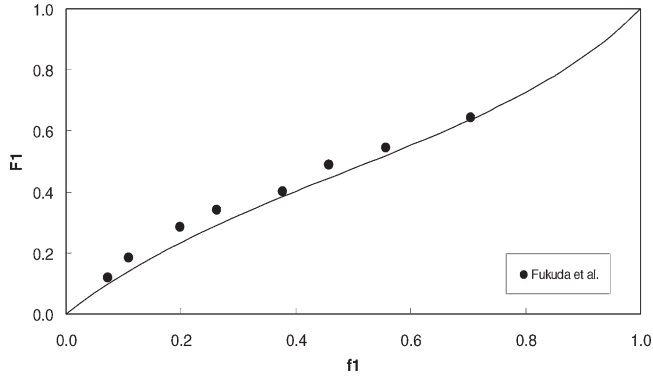

Figure 4.
Plot of ST mole fraction in copolymer (F_1) as a function of ST mole fraction in the monomer phase (f_1) estimated at 40 °C. Copolymer composition curve is the prediction of the terminal copolymerization model with computational monomer reactivity ratios $r_1 = 0.53$ and $r_2 = 0.68$. The filled circles are the experimental rotating-sector data from Fukuda et al.[10]

composition and propagation rate coefficients. In the latter case, the calculated curves in Figure 5 prove clearly the superior performance of the implicit penultimate model.

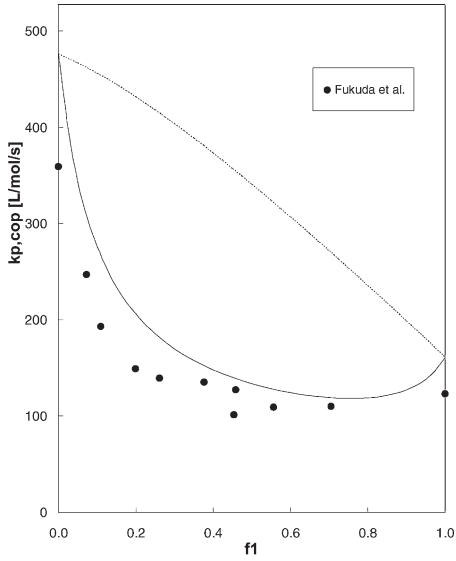

Figure 5.
Copolymer propagation rate coefficients ($k_{p,cop}$) as a function of ST monomer mole fraction (f_1) estimated at 40 °C. The lines represent the predictions of TM and IPUE using computational parameters ($r_1 = 0.53$, $r_2 = 0.68$, $s_1 = 0.23$, $s_2 = 0.99$, $k_{p111} = 161\text{L} \cdot \text{mol}^{-1} \cdot \text{s}^{-1}$[2c] and $k_{p222} = 476\text{L} \cdot \text{mol}^{-1} \cdot \text{s}^{-1}$[27]). The filled circles are the experimental rotating-sector data from Fukuda et al.[10]

Conclusion

In this work several mechanisms and reaction paths involved in free radical polymerizations were studied through a computational approach based on Density Functional Theory (DFT).

Different reaction steps have been examined: initiation, propagation, backbiting and beta-scission; moreover, propagation in copolymer systems was also studied. In all cases, the computational method is able to reproduce with good accuracy the experimental data, with errors usually smaller than the experimental ones. Therefore, the computational approach applied here can be considered an effective semi-quantitative tool to predict rate coefficients in polymeric systems. From the applicative point of view, such methods are expected to provide unique insights in secondary reactions in homopolymerization and in cross-propagation in copolymerization.

[1] a) S. Beuermann, M. Buback, P. Hesse, R. A. Hutchinson, S. Kukucova, I. Lacik, *Macromolecules* **2008**, *41*, 3513; b) M. Stach, I. Lacik, D. Chorvat, M. Buback, P. Hesse, R. A. Hutchinson, L. Tang, *Macromolecules* **2008**, *41*, 5174; c) M. Buback, F. Gunzler, G. T. Russell, P. Vana, *Macromolecules* **2009**, *42*, 652; d) K. Liang,

M. Dossi, D. Moscatelli, R. A. Hutchinson, *Macromolecules* **2009**, *42*, 7736; e) R. Siegmann, A. Jelicic, S. Beuermann, *Macromol. Chem. Phys.* **2010**, *211*, 546.
[2] a) O. F. Olaj, I. Bitai, F. Hinkelmann, *Makromol. Chem.* **1987**, *188*, 1689; b) O. F. Olaj, I. Schnollbitai, *Eur. Polym. J.* **1989**, *25*, 635; c) M. Buback, R. G. Gilbert, R. A. Hutchinson, B. Klumpermann, F. D. Kuchta, K. F. O'Driscoll, G. T. Russell, J. Schweer, *Macromol. Chem. Phys.* **1995**, *196*, 3267; d) S. Beuermann, M. Buback, T. P. Davis, R. G. Gilbert, R. A. Hutchinson, O. F. Olaj, G. T. Russell, J. Schweer, A. M. van Herk, *Macromol. Chem. Phys.* **1997**, *198*, 1545; e) S. Beuermann, M. Buback, T. P. Davis, R. G. Gilbert, R. A. Hutchinson, A. Kajiwara, B. Klumpermann, G. T. Russell, *Macromol. Chem. Phys.* **2000**, *201*, 1355; f) S. Beuermann, M. Buback, T. P. Davis, N. Garcia, R. G. Gilbert, R. A. Hutchinson, A. Kajiwara, M. Kamachi, I. Lacik, G. T. Russell, *Macromol. Chem. Phys.* **2003**, *204*, 1338; g) J. M. Asua, S. Beuermann, M. Buback, P. Castignolles, B. Charleux, R. G. Gilbert, R. A. Hutchinson, J. R. Leiza, A. N. Nikitin, J. P. Vairon, A. M. van Herk, *Macromol. Chem. Phys.* **2004**, *205*, 2151; h) W. Wang, R. A. Hutchinson, *Macromolecules* **2008**, *41*, 9011; i) J. Barth, M. Buback, P. Hesse, T. Sergeeva, *Macromolecules* **2009**, *42*, 481; j) M. Stach, I. Lacik, P. Kasak, D. Chorvat, A. J. Saunders, S. Santanakrishnan, R. A. Hutchinson, *Macromolecular Chemistry and Physics* **2010**, *211*, 580.
[3] A. N. F. Peck, R. A. Hutchinson, *Macromolecules* **2004**, *37*, 5944.
[4] a) J. P. A. Heuts, R. G. Gilbert, L. Radom, *Macromolecules* **1995**, *28*, 8771; b) J. P. A. Heuts, R. G. Gilbert, L. Radom, *J. Phys. Chem.* **1996**, *100*, 18997; c) H. Fischer, L. Radom, *Angew. Chem. Int. Ed.* **2001**, *40*, 1340; d) V. Van Speybroeck, K. Van Cauter, B. Coussens, M. Waroquier, *ChemPhysChem* **2005**, *6*, 180; e) E. I. Izgorodina, M. L. Coote, *Chem. Phys.* **2006**, *324*, 96; f) D. Moscatelli, C. Cavallotti, M. Morbidelli, *Macromolecules* **2006**, *39*, 9641; g) I. Degirmeci, et al., *M. Macromolecules* **2007**, *40*, 9599; h) D. Moscatelli, M. Dossi, C. Cavallotti, G. Storti, *Macromol. Symp.*, **2007**, *259*, 337; i) X. Yu, J. Pfaendtner, L. J. Broadbelt, *J. Phys. Chem. A* **2008**, *112*, 6772; j) I. Degirmeci, V. Van Speybroeck, M. Waroquier, *Macromolecules* **2009**, *42*, 3033; k) X. Yu, S. E. Levine, L. J. Broadbelt, *Macromolecules* **2008**, *41*, 8242; l) M. Dossi, K. Liang, R. A. Hutchinson, D. Moscatelli, *J. Phys. Chem B* **2010**, *114*, 4213; m) M. Dossi, G. Storti, D. Moscatelli, *Macromol. Theory Simul.* **2010**, *19*, 170; n) M. Dossi, G. Storti, D. Moscatelli, *Macromol. Symp.*, **2010**, *289*, 119.
[5] G. Odian, ''*Principle of polymerization*'', J. Wiley & Sons, New York 2004.
[6] R. S. Lehrle, C. S. Pattenden, *Polym. Degrad. Stab.* **1999**, *63*, 153.
[7] A. N. Nikitin, R. A. Hutchinson, M. Buback, P. Hesse, *Macromolecules* **2007**, *40*, 8631.
[8] M. Buback, P. Hesse, T. Junkers, T. Sergeeva, T. Theis, *Macromolecules* **2008**, *41*, 288.
[9] F. R. Mayo, F. M. Lewis, *J. Am. Chem. Soc.* **1944**, *66*, 1594.
[10] T. Fukuda, Y.-D. Ma, H. Inagaki, *Macromolecules*, **1985**, *18*, 17.
[11] Y. D. Ma, Y. C. Won, K. Kubo, T. Fukuda, *Macromolecules*, **1993**, *26*, 6766.
[12] A. D. Becke, *J. Chem. Phys.* **1993**, *98*, 5648.
[13] C. Lee, W. Yang, R. G. Parr, *Phys. Rev. B* **1988**, *37*, 785.
[14] M. W. Wong, L. Radom, *J. Phys. Chem. A* **1998**, *102*, 2237.
[15] V. Van Speybroeck, D. Van Neck, M. Waroquier, S. Wauters, M. Saeys, G. B. Marin, *J. Phys. Chem. A* **2000**, *104*, 10939.
[16] R. Gomez-Balderas, M. L. Coote, D. J. Henry, L. Radom, *J. Phys. Chem. A* **2004**, *108*, 2874.
[17] M. L. Coote, *J. Phys. Chem. A* **2004**, *108*, 3865.
[18] C. Peng, P. Y. Ayala, H. B. Schlegel, M. J. Frisch, *J. Comp. Chem.* **1996**, *17*, 49.
[19] M. K. Sabbe, M. F. Reyniers, V. Van Speybroeck, M. Waroquier, G. B. Marin, *ChemPhysChem* **2008**, *9*, 124.
[20] P. Vansteenkiste, V. Van Speybroeck, G. B. Marin, M. Waroquier, *J. Phys. Chem. A* **2003**, *107*, 3139.
[21] P. Vansteenkiste, V. Van Neck, V. Van Speybroeck, M. Waroquier, *J. Chem Phys.* **2006**, *124*, Art. N°044314.
[22] Gaussian 03, Revision C.02, M. J. Frisch, G. W. Trucks, H. B. Schlegel, G. E. Scuseria, M. A. Robb, J. R. Cheeseman, J. A. Montgomery, Jr., T. Vreven, K. N. Kudin, J. C. Burant, J. M. Millam, S. S. Iyengar, J. Tomasi, V. Barone, B. Mennucci, M. Cossi, G. Scalmani, N. Rega, G. A. Petersson, H. Nakatsuji, M. Hada, M. Ehara, K. Toyota, R. Fukuda, J. Hasegawa, M. Ishida, T. Nakajima, Y. Honda, O. Kitao, H. Nakai, M. Klene, X. Li, J. E. Knox, H. P. Hratchian, J. B. Cross, V. Bakken, C. Adamo, J. Jaramillo, R. Gomperts, R. E. Stratmann, O. Yazyev, A. J. Austin, R. Cammi, C. Pomelli, J. W. Ochterski, P. Y. Ayala, K. Morokuma, G. A. Voth, P. Salvador, J. J. Dannenberg, V. G. Zakrzewski, S. Dapprich, A. D. Daniels, M. C. Strain, O. Farkas, D. K. Malick, A. D. Rabuck, K. Raghavachari, J. B. Foresman, J. V. Ortiz, Q. Cui, A. G. Baboul, S. Clifford, J. Cioslowski, B. B. Stefanov, G. Liu, A. Liashenko, P. Piskorz, I. Komaromi, R. L. Martin, D. J. Fox, T. Keith, M. A. Al-Laham, C. Y. Peng, A. Nanayakkara, M. Challacombe, P. M. W. Gill, B. Johnson, W. Chen, M. W. Wong, C. Gonzalez, J. A. Pople, Gaussian, Inc., Wallingford, CT **2004**.
[23] W. L. DeLano, *The PyMOL Molecular Graphics System*, DeLano Scientific, San Carlos, CA 2002.
[24] M. Okubo, T. Mori, *Macromol. Symp.* **1990**, *31*, 143.
[25] S. J. Li, F. P. Wu, M. Z. Li, E. J. Wang, *Polymer.* **2005**, *46*, 11934.
[26] M. Buback, C. Kurz, C. Schmaltz, *Macromol. Chem. Phys.* **1998**, *199*, 1721.
[27] S. Beuermann, M. Buback, T. P. Davis, R. G. Gilbert, R. A. Hutchinson, et al., *Macromol. Chem. Phys.*, **1997**, *198*, 1545.

[28] T. Junkers, S. P. S. Koo, C. Barner-Kowollik, *Polym. Chem.* **2010**, *1*, 438.
[29] Y. Ma, P. Kim, K. Kubo, T. Fukuda, *POLYMER*, **1994**, *35*, 1375.
[30] M. Buback, C. Kurz, *Macromol. Chem. Phys.* **1998**, *199*, 2301.
[31] R. A. Hutchinson, D. A. Paquet, J. H. McMinn, S. Beuermann, R. E. Fuller, C. Jackson, *DECHEMA Monogr.* **1995**, *131*, 467.
[32] D. Cuccato, M. Dossi, D. Moscatelli, G. Storti, *Macromol. Symp.*, **2010**, submitted.
[33] K. Van Cauter, B. J. Van Den Bossche, V. Van Speybroeck, M. Waroquier, *Macromolecules* **2007**, *40*, 1321.
[34] M. L. Coote, L. P. M. Johnston, T. P. Davis, *Macromolecules* **1997**, *30*, 8191.
[35] R. X. E. Willemse, A. M. van Herk, *J. AM. CHEM. SOC.* **2006**, *128*, 4471.

